

# SAM-TTT: Segment Anything Model via Reverse Parameter Configuration and Test-Time Training for Camouflaged Object Detection

Zhenni Yu

College of Computer Science and Artificial Intelligence,  
Wenzhou University  
Wenzhou, Zhejiang, China  
College of Computer Science and Technology, Tongji  
University  
Shanghai, China  
zhenn\_yu@163.com

Guobao Xiao\*

College of Computer Science and Technology, Tongji  
University  
Shanghai, China  
x-gb@163.com

Li Zhao

College of Information Science and Technology, Zhejiang  
Shuren University  
Hangzhou, Zhejiang, China  
zhaoli@zjsru.edu.cn

Xiaoqin Zhang\*

College of Computer Science and Artificial Intelligence,  
Wenzhou University  
Wenzhou, Zhejiang, China  
zhangxiaoqinnan@gmail.com

## Abstract

This paper introduces a new Segment Anything Model (SAM) that leverages reverse parameter configuration and test-time training to enhance its performance on Camouflaged Object Detection (COD), named SAM-TTT. While most existing SAM-based COD models primarily focus on enhancing SAM by extracting favorable features and amplifying its advantageous parameters, a crucial gap is identified: insufficient attention to adverse parameters that impair SAM's semantic understanding in downstream tasks. To tackle this issue, the Reverse SAM Parameter Configuration Module is proposed to effectively mitigate the influence of adverse parameters in a train-free manner by configuring SAM's parameters. Building on this foundation, the T-Visioner Module is unveiled to strengthen advantageous parameters by integrating Test-Time Training layers, originally developed for language tasks, into vision tasks. Test-Time Training layers represent a new class of sequence modeling layers characterized by linear complexity and an expressive hidden state. By integrating two modules, SAM-TTT simultaneously suppresses adverse parameters while reinforcing advantageous ones, significantly improving SAM's semantic understanding in COD task. Our experimental results on various COD benchmarks demonstrate that the proposed approach achieves state-of-the-art performance, setting a new benchmark in the field.

\*corresponding authors.

Permission to make digital or hard copies of all or part of this work for personal or classroom use is granted without fee provided that copies are not made or distributed for profit or commercial advantage and that copies bear this notice and the full citation on the first page. Copyrights for components of this work owned by others than the author(s) must be honored. Abstracting with credit is permitted. To copy otherwise, or republish, to post on servers or to redistribute to lists, requires prior specific permission and/or a fee. Request permissions from permissions@acm.org.

MM '25, Dublin, Ireland

© 2025 Copyright held by the owner/author(s). Publication rights licensed to ACM.  
ACM ISBN 979-8-4007-2035-2/2025/10  
<https://doi.org/10.1145/3746027.3755291>

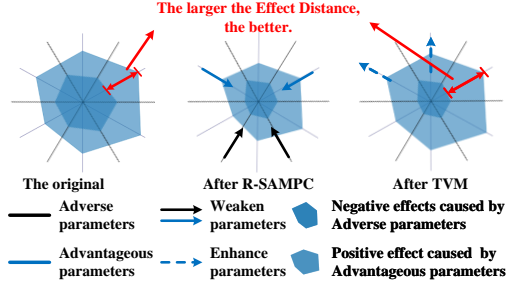


**Figure 1:** Conceptual Diagram of SAM-TTT from the Perspective of Effect Distance. The roles of the R-SAMPC and TVM. R-SAMPC weakens the adverse and advantageous parameters, while TVM strengthens the advantageous parameters.

## CCS Concepts

- Computing methodologies → Object detection; Computer vision; Artificial intelligence.

## Keywords

Camouflaged Object Detection, Segment Anything Model, Test-Time Training, Parameter Configuration

## ACM Reference Format:

Zhenni Yu, Li Zhao, Guobao Xiao, and Xiaoqin Zhang. 2025. SAM-TTT: Segment Anything Model via Reverse Parameter Configuration and Test-Time Training for Camouflaged Object Detection. In *Proceedings of the 33rd ACM International Conference on Multimedia (MM '25), October 27–31, 2025, Dublin, Ireland*. ACM, New York, NY, USA, 9 pages. <https://doi.org/10.1145/3746027.3755291>

## 1 Introduction

Segment Anything Model (SAM) [20] is undergoing rapid development. Its impressive zero-shot capabilities enable good results in various downstream tasks while also saving training costs, leading

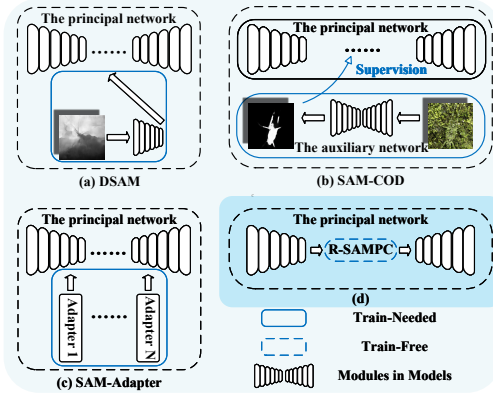


**Figure 2: A comparative analysis of solutions to mitigate the semantic deficiency encountered when applying SAM to COD.**

to widespread utilization and exploration. Currently, SAM faces the issue of semantic deficiency as it progresses towards downstream tasks [27]. In the specific downstream task of Camouflaged Object Detection (COD), semantic deficiency issues manifest in the segmentation masks not aligning with the intended semantics [17]. This phenomenon suggests that SAM produces object-biased fine-grained semantic responses in COD [3]. The underlying cause is SAM’s zero-shot capabilities stem from the SA-1B dataset. The SA-1B dataset exhibits a domain gap compared to the COD dataset. Several studies have been conducted to address this issue. SAM-COD [3] produces a preliminary mask using additional network, which contains an initial understanding, to correct the above errors by calculating the semantic entropy. SAM-Adapter [4] utilizes adapter technology to integrates domain knowledge to SAM. Aware of the limitations of RGB modality, DSAM [39] adds depth information to correct the semantic missing. However, all these methods require the integration of additional coding modules to fulfill their objectives, which adds complexity to their implementation. A deeper underlying reason is that most researchers focus on introducing semantic information to compensate for its absence, while few pay attention to the adverse parameters within SAM that contribute to the generation of erroneous semantic information.

To solve these problems, a new SAM-based model is proposed for COD, named SAM-TTT. SAM-TTT integrates the Reverse SAM Parameter Configuration Module (R-SAMPC) and T-vision Module (TVM) to strengthen SAM’s performance on COD. SAM-TTT focuses on the impact of parameters in SAM and introduces a conceptual metric called **Effect Distance**, which represents the quality of parameters—it increases as beneficial parameters are enhanced and detrimental ones are suppressed. SAM-TTT configures the parameters of SAM in a new way of widening the Effect Distance, shown in Figure 1. This concept derives from the unique working mechanism of R-SAMPC. Unlike existing approaches that use additional coding modules to introduce semantic information, as illustrated in (a), (b), (c) of Figure 2, R-SAMPC solves the problem in a train-free way, as shown in (d) of Figure 2. It is through a designed randomly initialized convolution module that does not update to loosen the constraints on the parameters, ultimately reducing the

impact of adverse parameters in SAM for COD. R-SAMPC configures the parameters in this novel way and mitigates the semantic deficiency caused by adverse parameters. It’s used during training but not during inference. R-SAMPC focuses on weakening the parameters, which is contrary to the previous approaches that emphasized enhancing the parameters; thus, it is named “Reverse”. From another perspective, R-SAMPC is viewed as a random mask at the parameter level, corresponding to random initialization. The random mask is able to suppress strong responses [21]. Chen et al. [2] diverted the model’s attention across the entire object by partially occluding the labeled regions, rather than focusing on the most distinctive parts. R-SAMPC disturbs the part of the model that is highly responsive in a train-free way and forces the model to focus on the whole. R-SAMPC addresses the semantic deficiency issues caused by SAM in COD by weakening the adverse parameters in a train-free manner.

Furthermore, R-SAMPC introduces a certain level of disruption for advantageous parameters. TVM is proposed to extract favorable features to compensate for this interference. TVM adopts TTT-Linear, an instantiation of the TTT layer [32]. TTT is an RNN layer with linear complexity and a highly expressive hidden state. TVM incorporates TTT into computer vision to extract advantageous features. TTT lets the hidden state itself be a weight. This approach breaks the restriction that their representation in long context is limited by the expressive power of hidden states [32].

SAM-TTT proposes R-SAMPC to mitigate the impact of adverse factors and designs TVM to extract advantageous factors from the interference caused by R-SAMPC. Because the two modules in the serial structure will have contradictory effects (weakening and strengthening) to cancel out the effect. In order to fuse the functions of the two modules, SAM-TTT is designed as a structure of first parallel and then fusion. Unlike the serial structure, two modules do not interfere with each other in the parallel structure. Finally, in the fusion stage, the function of the two modules is combined. Dilated and grouped convolutions are employed to effectively capture multi-scale contextual information, enabling more precise fusion. Overall, SAM-TTT configures the parameters of SAM by broadening the Effect Distance between advantageous and adverse parameters in the model, partially addressing the semantic deficiency in SAM used for COD. Our contributions are summarized as follows:

- SAM-TTT is proposed for COD. SAM-TTT is a new SAM-based model that is the first to focus on expanding the Effect Distance between advantageous and adverse parameters, addressing the issue of semantic deficiency when applying SAM to COD.
- Two efficient designs are proposed in SAM-TTT: R-SAMPC and TVM. R-SAMPC is a SAM parameter configuration module that mitigates the effects of adverse parameters in SAM in a train-free way. TVM extracts advantageous parameters to compensate for the parameter interference caused by R-SAMPC .
- The performance of SAM-TTT is verified on COD benchmark datasets. SAM-TTT outperforms the existing SOTA methods. It can be concluded that SAM-TTT reaches the cutting-edge in this domain.

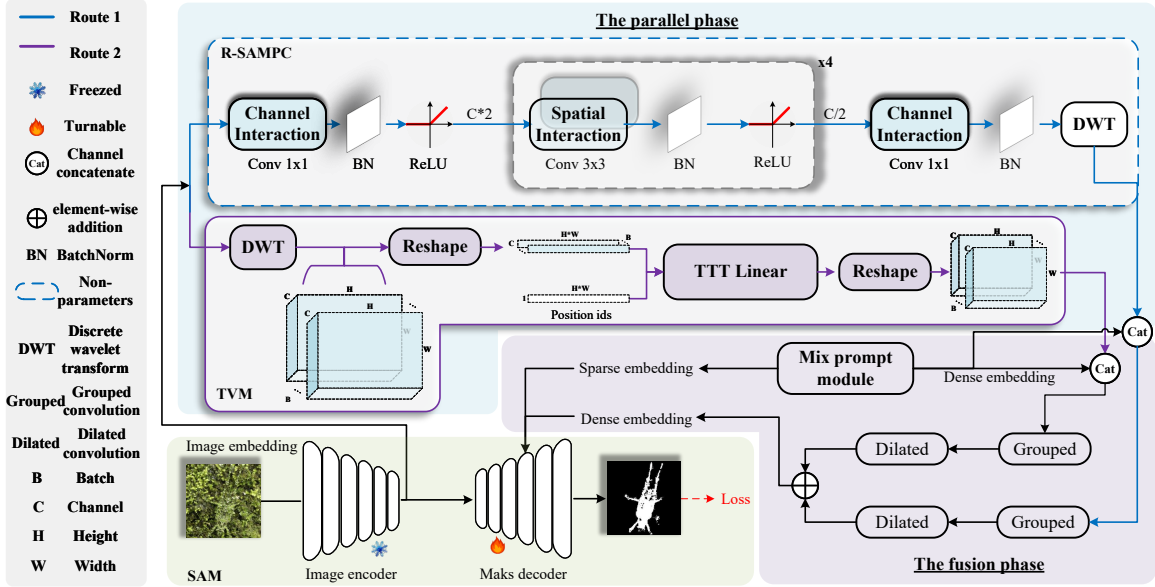


**Figure 3:** Overview of our SAM-TTT framework: the Reverse SAM Parameter Configuration Module (R-SAMPC) and the T-vision Module (TVM). In the parallel phase, R-SAMPC and TVM operate independently, while in the fusion phase, the effectiveness of both modules is integrated.

## 2 Related Work

### 2.1 Camouflaged Object Detection

In nature, animals use camouflage as a defense strategy to evade predators [5]. COD [9, 37] is the process of identifying and segmenting camouflaged objects that blend into their surroundings. Many studies tackle this problem from multiple perspectives. They focus on gradient analysis [16], proactive template learning [1], boundary detection [23, 31, 33, 44], depth cues [24, 39], zoom-out strategies [29], predation techniques [8, 18], and other related approaches [38, 41]. Today's cutting-edge methods continue to explore these aspects more deeply. FSEL [34] highlights that previous methods overlook critical information found between high-frequency and low-frequency ranges. It integrates both global frequency and local spatial features to improve the detection of camouflaged objects. ZoomNeXt [30] mimics human behavior (i.e., zooming in and out) when observing vague images and videos. RISNet [36] extends classic COD to agricultural domains. It employs multiscale receptive fields and integrates depth features to capture information about camouflage crops of varying sizes and spatial locations. It grounds the COD task in agricultural application. Due to the huge human effort required by the labels required for full supervision, some semi-supervised methods developed. Chen et al. [2] proposed a novel point-based learning paradigm for the challenging COD task. GenSAM [13] reasons visual prompts based on the semantic information from a generic text prompt of cross-modal large language mode.

### 2.2 Camouflaged Object Detection based SAM

As a novel foundation model, SAM is trained on a vast dataset and demonstrates impressive zero-shot capabilities. However, due to the domain gap between the data set trained by SAM and the data set of COD, the accuracy of SAM is inevitably reduced when it is applied to the field of COD [17]. Similarly, Tang et al. [35] directly studied COD and highlighted that SAM performs suboptimally on the COD task. One of the more specific embodiments is the lack of segmentation semantics [3]. This makes the internal segmentation of the camouflage target incomplete. He et al. [12] used sparse annotations from SAM as guidance for mask segmentation during model training. SAM-Adapter [4] integrates domain-specific information or visual prompts into the segmentation network using straightforward yet effective adapters. DSAM [39] refines the mask generated by SAM using depth cues to give semantic cues. SAM-COD [3] uses masks generated by an auxiliary network, which contain the initial semantics, to correct the masks predicted by SAM. COMProptter [43] employs a mixed prompt approach, integrating both box prompts and boundary prompts to deliver more reliable semantic information. However, this method depends on the integration of an external auxiliary network or modules to tackle the challenge of internal semantic deficiency. While this approach can enhance performance, it also introduces additional parameters and computational complexity, which may impact efficiency. And it does not solve the problem of missing semantics of SAM applied to COD from the root, SAM itself.

### 3 Methodology

#### 3.1 Overall Architecture

SAM-TTT consists of the Reverse SAM Parameter Configuration Module (R-SAMPC) and the T-visioner Module (TVM), shown in Figure 3. The image embedding is derived from the frozen image encoder of SAM. It possesses strong zero-shot capabilities, but it also contains knowledge that may not align with COD. To address this, SAM-TTT is proposed. It actively weakens knowledge that is adverse for COD and strengthens knowledge that is advantageous. The network is structured with an initial parallel design followed by a fusion stage, aiming to maximize the distance between advantageous and adverse parameters. In the parallel phase, R-SAMPC and TVM act independently and do not interfere with each other, avoiding the possible effect cancellation of the weakening and the enhancing effects. In the fusion phase, the mix prompt method of COMPromter is adopted. Features from R-SAMPC and TVM are fused into the hybrid prompts to guide the mask decoder. The issue of semantic deficiency of SAM applied to COD is alleviated.

#### 3.2 Reverse SAM Parameter Configuration Module

The Reverse SAM Parameter Configuration Module (R-SAMPC) is designed to configure the parameters of SAM in a manner that increases the distance between adverse and advantageous features. In essence, R-SAMPC is a convolutional module that does not update parameters, functioning as a train-free method. It weakens the parameters in SAM that are not conducive to COD task, and obviously alleviates the lack of semantics of SAM applied to COD. Formally, this module can also be seen as a dropout, which only participates during training and not during inference. Traditional dropout either zeros out neurons or adds Gaussian noise. Unlike traditional dropout, R-SAMPC consists of a series of convolutional layers, Batch Normalization, and ReLU activation. R-SAMPC is only initialized during training and its parameters are not updated. So this module is trained in a train-free manner. Through R-SAMPC, image embedding disturbs the original parameters to a certain extent. R-SAMPC ( $\mathcal{F}$ ) is expressed as follows:

$$\mathcal{F} = CI_R(SI(CI_D(em_I))) \quad (1)$$

where  $CI_D$  represents channel interaction using a 1x1 convolution with BatchNorm and ReLU, which doubles the number of channels.  $SI$  denotes spatial interaction using the four layers of 3x3 convolution with BatchNorm and ReLU.  $CI_R$  represents channel interaction using a 1x1 convolution with BatchNorm, which reduces the number of channels to one-half of the original.  $em_I$  denotes embedding from image encoder. The function of  $CI_D$  and  $CI_R$  is to facilitate communication of the image embedding across the channel dimension.  $SI$  enables simple communication over the spatial dimension. The simple convolutional combination in R-SAMPC is designed to introduce noise, with the aim of directly reducing the influence of adverse parameters in SAM. From this point of view, R-SAMPC can be seen as a mask for parameters. While previous works apply occlusion to the prediction mask [3], additional modules will be used to map the occlusion on the mask level to the parameter level. Other methods use the auxiliary network to correct mistakes (Figure 2 (a), (b), (c)). Thus, R-SAMPC adds noise more directly and

does not require additional subsequent computations (Figure 2 (d)). From another point of view, adding random masks can force the model to focus on the overall objective by shifting its attention away from the highest parts [2]. Our R-SAMPC is exactly a parametric manifestation of this phenomenon. R-SAMPC is applied to *route1* in the parallel phase participating in SAM-TTT.

#### 3.3 T-visioner Module

R-SAMPC weakens knowledge in image embedding that is detrimental to COD. At the same time, the knowledge that it benefits COD is also weakened inevitably. So, in another route in SAM-TTT, TVM is designed to emphasize the knowledge that SAM is beneficial for COD. Self-attention excels at handling long-range dependencies but comes with quadratic complexity. In contrast, traditional RNN layers have linear complexity, though their ability to model long-term context is constrained by the limited expressive capacity of their hidden states. Test-Time Training (TTT) [32] layers solves this problem. The core concept is to treat the hidden state as a machine learning model. An instantiation of TTT is introduced, called TTT-linear, into *Route2* in the parallel phase to reinforce dominant features. The challenge that needs to be overcome is how to bring TTT, which is an RNN layer, to the field of computer vision. As shown in Figure 3, the usage of DWT [11] in COMPromter is retained by us. DWT primarily captures diagonal high-frequency regions in an image, highlighting edges and subtle variations. DWT first extracts the high-frequency components of the image embedding and then adjusts the feature dimensions to comply with the requirements of the RNN layer. The process is as follows:

$$\text{reshape} : B \times C \times W \times H \longrightarrow B \times (W \times H) \times C \quad (2)$$

Additionally, a positional encoding is generated. Its contents are integers from 0 to  $W \times H - 1$ . The dimensions of it is as followed:

$$\text{Position encoding} : 1 \times (W \times H - 1) \quad (3)$$

After TTT-Liner, the shape will change the original dimension.

$$\text{reshape} : B \times (W \times H) \times C \longrightarrow B \times C \times W \times H \quad (4)$$

The role of TVM is to compensate for the interference caused by R-SAMPC on the advantageous parameters.

## 4 Experiments

### 4.1 Dataset

Experiments are conducted on three widely used datasets, namely CAMO [22], COD10K [8], and NC4K [26]. This aims to evaluate the impact of SAM-TTT on the task of COD. CAMO contains a total of 1250 images, which are randomly divided into a training set of 1000 images and a test set of 250 images. COD10K includes 5066 images, with 3040 used for training and 2026 for testing. NC4K is a relatively large dataset, consisting of 4121 images in total. It is utilized as a test set in experiments to assess the generalization capability of SAM-TTT. Following Fan et al. [8], our study adopts that the dataset is composed of the train datasets of COD10K and CAMO, which are 3040 images and 1000 images, respectively. The remaining images of COD10K and CAMO and the entire NC4K dataset are used as the test dataset.

**Table 1: Quantitative results on three different datasets of CAMO, COD10K, and NC4K.**  $\uparrow$  indicates the higher the score the better and  $\downarrow$  indicates the lower the score the better. The highest and second-highest scores are bolded, while the third score is underlined.

Dataset	Metric	SINet	Zoo	Seg	DG	MSC	Hit	PR	RIS	Camo	FSEL	PRBE	SAM	SAMA	D	COMPr	<b>Ours</b>
		V2	mNet	MaR	Net	AFNet	Net	Net	Net	Focus				apter	SAM	ompter	
		2022	2022	2023	2023	2023	2023	2024	2024	2024	2024	2024	2023	2023	2024	2024	
CAMO	$F_\beta^\omega \uparrow$	0.743	0.752	0.742	0.769	0.828	0.801	0.831	0.827	<b>0.842</b>	<b>0.851</b>	0.837	0.606	0.765	0.794	0.819	<u>0.838</u>
	$S_\alpha \uparrow$	0.820	0.820	0.815	0.839	0.873	0.844	0.872	0.870	<u>0.873</u>	<b>0.885</b>	<b>0.876</b>	0.684	0.847	0.832	0.853	0.868
	$E_\phi \uparrow$	0.882	0.892	0.872	0.901	0.929	0.902	<u>0.922</u>	0.922	-	<b>0.942</b>	-	0.687	0.873	0.913	0.919	<b>0.935</b>
	$M \downarrow$	0.070	0.066	0.071	0.057	0.046	0.057	0.050	0.050	<b>0.043</b>	<b>0.040</b>	<u>0.045</u>	0.132	0.070	0.061	0.054	<u>0.045</u>
COD 10K	$F_\beta^\omega \uparrow$	0.680	0.729	0.724	0.693	0.775	0.798	<b>0.803</b>	<u>0.802</u>	<u>0.802</u>	<b>0.805</b>	0.793	0.701	0.801	0.760	0.779	<b>0.805</b>
	$S_\alpha \uparrow$	0.815	0.838	0.833	0.822	0.865	0.868	0.873	0.873	<b>0.877</b>	0.867	0.783	<b>0.883</b>	0.846	0.861	<u>0.874</u>	
	$E_\phi \uparrow$	0.887	0.911	0.895	0.896	0.927	0.932	<u>0.935</u>	0.930	-	<b>0.938</b>	-	0.798	0.918	0.921	0.933	<b>0.942</b>
	$M \downarrow$	0.037	0.029	0.033	0.033	<u>0.024</u>	<u>0.024</u>	0.025	0.028	<b>0.021</b>	<b>0.023</b>	<b>0.021</b>	0.049	0.025	0.033	0.026	0.027
NC4K	$F_\beta^\omega \uparrow$	0.770	0.784	0.781	0.784	0.839	0.825	0.832	0.823	<b>0.853</b>	0.836	<b>0.845</b>	0.696	-	0.826	0.840	<u>0.837</u>
	$S_\alpha \uparrow$	0.847	0.853	0.841	0.857	<b>0.887</b>	0.870	<u>0.885</u>	0.879	<b>0.889</b>	<b>0.887</b>	<b>0.887</b>	0.767	-	0.871	0.880	0.884
	$E_\phi \uparrow$	0.903	0.912	0.905	0.911	<u>0.935</u>	0.921	<u>0.935</u>	0.927	-	<b>0.940</b>	-	0.776	-	0.932	<u>0.935</u>	<b>0.943</b>
	$M \downarrow$	0.048	0.043	0.046	0.042	0.032	0.039	<b>0.029</b>	0.033	<b>0.030</b>	<b>0.028</b>	0.031	0.078	-	0.040	0.036	0.031

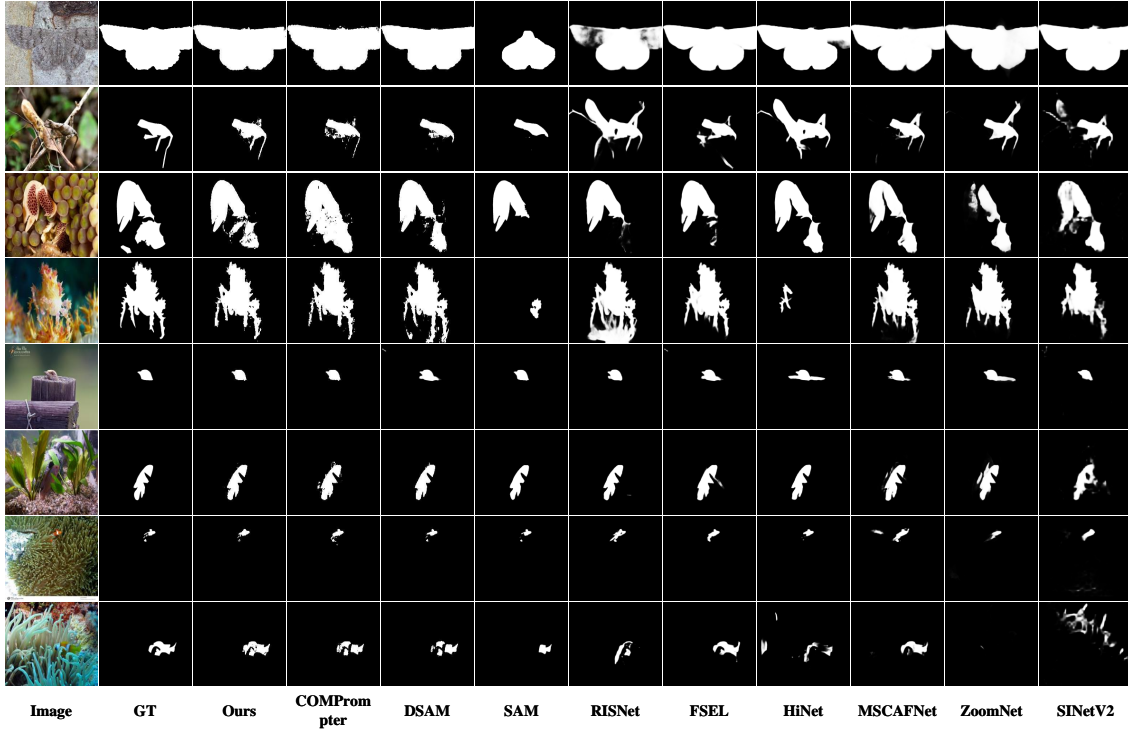


Figure 4: Comparison of our SAM-TTT and other methods on different types of samples. (Better to zoom in.)

## 4.2 Experimental Setup

**Implementation Details.** SAM-TTT is implemented using PyTorch, employing the Adam optimizer with a learning rate of  $1e^{-5}$ . The model is trained for 290 epochs to achieve optimal performance, taking around 24 hours to complete on an NVIDIA 3080TI GPU

with a batch size of 16. All input images are resized to  $1024 \times 1024$  using bilinear interpolation, scaling them up or down as needed. In addition, the input image data are truncated and normalized. This ensures the pixel values are in the appropriate range while maintaining the relative distribution relationship of the data.

**Table 2: Comparison of Network Complexity.** The parameters in parentheses represent the training parameters.

Models	Input size	Param (M)	Speed (fps)
SINetV2	352×352	26.98 (26.98)	50
DGNet	352×352	21.02 (21.02)	40
FSEL	416×416	67.13 (67.13)	31
SAM	1024×1024	91 (91)	2
SAM-TTT	1024×1024	96.32 (6.65)	3

**Evaluation Metrics.** Four metrics from COD10K [8] are adopted. These four metrics are commonly used and well-established in the field of COD: structure measure ( $S_\alpha$ ) [6], weighted F-measure ( $F_\beta^w$ ) [28], mean enhanced-alignment measure ( $E_\phi$ ) [7], and mean absolute error ( $M$ ). The structure measure quantifies the structural similarity between the predicted results and the actual segmented regions. The weighted F-measure combines precision and recall, and weights them. The enhanced-alignment measure evaluates the prediction result by comparing the alignment relationship between the predicted value and the actual value. The mean absolute error is a measure of the mean absolute error between the predicted value and the true value.

### 4.3 Comparisons with Cutting-Edge Methods

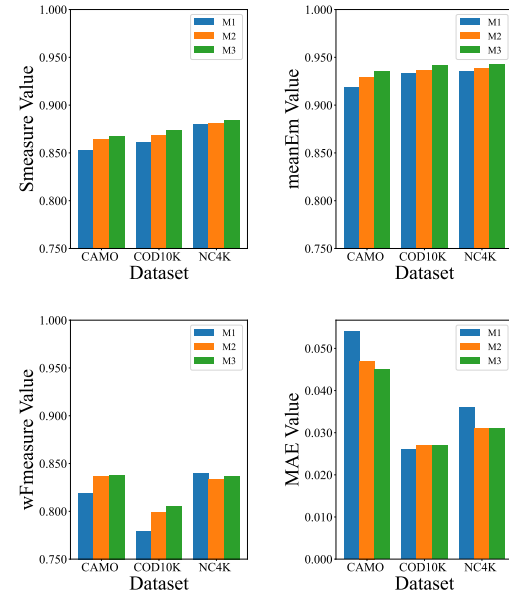
Here, data from top-performing models over the past three years is selected. To ensure a comprehensive comparison, both SAM-based models and non-SAM methods are included. SAM-TTT is compared with SAM [20] and other existing COD algorithms, such as SINetV2 [8], ZoomNet [29], SegMaR [18], DGNet [16], MSCAF-Net [25], HitNet [14], PRNet [15], RISNet [36], PNet [42], Camo-Focus [19], FSEL [34], SAM-Adapter [4], DSAM [39], COMPrompt [43]. The predictions of the competitors are disclosed by the authors or generated by models retrained using open-source code. The comparison results are presented in Table 1.

**Efficiency analysis.** Table 2 compares parameter counts and inference speed. Although SAM-TTT has a large total parameter size (96.32M), its trainable parameters are only 6.65M—about one-tenth of FSEL’s. This keeps computational overhead low while outperforming fully supervised methods under similar complexity.

**Quantitative Results.** The quantitative comparison results of the proposed algorithm and the other 15 methods on the three datasets are shown in Table 1. The 15 methods include both SAM-based models and non-SAM-based models. No one method has a completely significant advantage. Given the similar and competitive accuracy, the top three scores are highlighted across 12 metrics on three datasets. There exists some same score in top three score. The identical top scores reflect the intense level of competition. Among the top 2 scores, half of the differences are less than 0.3%. The table highlights that among the top three scores across 12 metrics, 6 metrics have overlapping data. SAM-TTT secures top-three positions in 8 out of 12 metrics, indicating a certain level of advancement. On CAMO, SAM-TTT performs slightly worse, likely due to enhanced generalization from SAM knowledge and R-SAMPC perturbations at the expense of learning ability. The high train-test ratio (1000:250) may further amplify this effect.

**Table 3: Ablation study results for each module of the proposed SAM-TTT on COD datasets.**  $P$  represents the average value of positive metrics, while  $N$  represents the average value of negative metrics.  $\uparrow$  indicates the higher the score the better and  $\downarrow$  indicates the lower the score the better.

Dataset	Metric	M1	M2	M3*	M3
CAMO	$F_\beta \uparrow$	0.819	0.836	0.837	0.838
	$S_\alpha \uparrow$	0.853	0.864	0.866	0.868
	$E_\phi \uparrow$	0.919	0.929	0.933	0.935
	$M \downarrow$	0.054	0.047	0.047	0.045
COD10K	$F_\beta \uparrow$	0.779	0.799	0.808	0.805
	$S_\alpha \uparrow$	0.861	0.869	0.873	0.874
	$E_\phi \uparrow$	0.933	0.937	0.941	0.942
	$M \downarrow$	0.026	0.027	0.026	0.027
NC4K	$F_\beta \uparrow$	0.840	0.833	0.839	0.837
	$S_\alpha \uparrow$	0.880	0.881	0.885	0.884
	$E_\phi \uparrow$	0.935	0.939	0.942	0.943
	$M \downarrow$	0.036	0.031	0.030	0.031
Average	$P \uparrow$	0.869	0.876	0.880	0.881
	$N \downarrow$	0.0387	0.0350	0.0343	0.0343

**Figure 5: Visualization of ablation experiments.** M1 denotes baseline, COMPrompt. M2 denotes baseline + R-SAMPC. M3 denotes baseline + R-SAMPC + TVM, which is SAM-TTT.

**Qualitative Results.** The visual comparisons of different methods on COD datasets are presented in Figure 4. The masks from various perspectives are selected, including tiny objects (Rows 5 and 7), small objects (Rows 6 and 8), large objects (Rows 1 and 3), occluded objects (Rows 5 and 6), and objects with fine structures (Row 2 and 4). In Rows 2 and 4, the details of the objects are

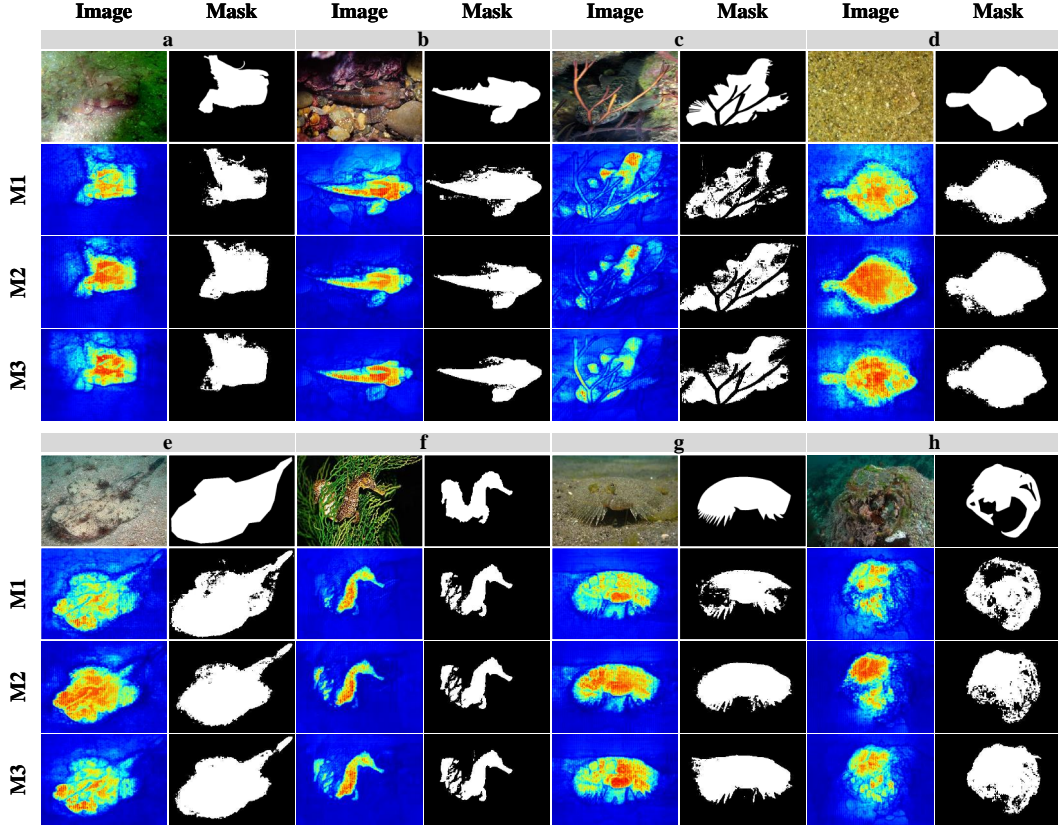


**Figure 6: Group-wise feature map, mask, image, and ground truth comparison based on ablation settings.  $M_1$  denotes baseline, COMPromter.  $M_2$  denotes baseline + R-SAMPC.  $M_3$  denotes baseline + R-SAMPC + TVM, which is SAM-TTT.**

clearly shown through SAM-TTT. In contrast, the other methods exhibit either over-segmentation or under-segmentation, leading to blurred details. The illustrated results show that SAM-TTT demonstrates a more detailed handling of fine features. Under occlusion, the model requires more semantic knowledge. In Rows 6, 7, and 8, SAM-TTT effectively distinguishes occlusions from objects and demonstrates more accurate segmentation. SAM-TTT provides a more comprehensive semantic understanding when addressing occlusion. A similar background can be beneficial for camouflaged objects. In Row 4, the background is similar to the object, making it challenging for many methods to detect the boundaries between the target and the background. However, SAM-TTT demonstrates superior discrimination in such cases, as shown in Row 4.

#### 4.4 Ablation study

Ablation experiments are conducted to evaluate the effectiveness of R-SAMPC and TVM. Specifically, R-SAMPC serves as a prerequisite for TVM. Four models are designed to demonstrate the effectiveness of R-SAMPC and TVM. COMPromter is chosen as the baseline model, referred to as  $M_1$ .  $M_2$  adds R-SAMPC and the corresponding fusion phase to  $M_1$ , while  $M_3$  incorporates TVM and the corresponding fusion phase based on  $M_2$ . In addition,  $M_3^*$  replaces TTT with Mamba [10] to assess the effectiveness of TTT.

The quantitative results of different models in SAM-TTT are provided, shown in Table 3. In order to better observe the accuracy gap between models, Table 3 is visualized as Figure 5. To observe the effect of R-SAMPC and TVM, the feature visualizations of  $M_1$ ,  $M_2$ ,  $M_3$  are compared with the final masks of this model, displayed in Figure 6. Finally, to confirm the rationality of R-SAMPC, an ablation experiment is performed on the rationality of R-SAMPC structure, which is shown in Table 4.

**Effectiveness of R-SAMPC.** The effectiveness of R-SAMPC is demonstrated by the gap between  $M_1$  and  $M_2$ . As shown in Figure 5,  $M_2$  achieves an overall improvement compared to  $M_1$ , with particularly notable gains in the three positive metrics. The effectiveness of R-SAMPC is analyzed based on average metrics.  $M_2$  achieves an average improvement of 0.6% in  $S_\alpha$ , 1.0% in  $F_\beta^\omega$ , 0.6% in  $E_\phi$  across three datasets. The negative metric,  $M$  is reduced by 0.37%. Overall,  $M_2$  shows a 0.7% improvement in positive metrics compared to  $M_1$ . To clarify the role of R-SAMPC, it is analyzed from the perspective of feature maps. Figure 6 lists a total of 8 groups of feature maps and mask comparison maps. From the feature maps of  $M_1$  in groups a, e, g and h, it is obvious that there are low response areas caused by semantic errors inside the object in  $M_1$ . Part of this low response is reflected in the final prediction map being abnormal hollowing inside the object (see  $M_1$ 's masks of groups a, e, g and

**Table 4:** Ablation study results for R-SAMPC.  $L0$  denotes COMPromter.  $L1$  denotes baseline + a layer of convolutional combinations.  $L2$  denotes two layers.  $L3$  denotes three layers.  $L4$  denotes four layers.  $L4 + \epsilon$  denotes  $L4 +$  channel scaling.  $P$  represents the average value of positive metrics, while  $N$  represents the average value of negative metrics. The best data is marked bold, and the second best data is underlined.  $\uparrow$  indicates the higher the score the better and  $\downarrow$  indicates the lower the score the better.

Setting	CAMO					COD10K					NC4K					Average				
	$S_\alpha \uparrow$	$F_\beta^\omega \uparrow$	$E_\phi \uparrow$	$F_m \uparrow$	$E_x \uparrow$	$M \downarrow$	$S_\alpha \uparrow$	$F_\beta^\omega \uparrow$	$E_\phi \uparrow$	$F_m \uparrow$	$E_x \uparrow$	$M \downarrow$	$S_\alpha \uparrow$	$F_\beta^\omega \uparrow$	$E_\phi \uparrow$	$F_m \uparrow$	$E_x \uparrow$	$M \downarrow$	$P$	$N$
$L0$	0.853	0.819	0.919	0.843	0.931	0.054	0.861	0.779	0.933	0.806	0.945	0.026	0.880	0.840	0.935	0.862	0.946	0.036	0.8768	0.0387
$L1$	0.863	0.834	0.928	0.855	0.938	0.048	0.868	0.797	0.937	0.823	0.948	0.027	0.880	0.831	0.938	0.853	0.948	0.031	0.8827	0.0353
$L2$	0.861	0.831	0.927	0.852	0.937	0.049	0.868	0.797	0.937	0.821	0.948	0.027	0.881	0.831	0.939	0.852	0.948	0.032	0.8820	0.0360
$L3$	0.864	0.834	0.929	0.855	0.940	0.048	0.869	0.799	0.937	0.824	0.948	0.027	0.881	0.833	0.939	0.854	0.949	0.031	0.8837	0.0353
$L4$	0.864	0.835	0.930	0.855	0.94	0.047	0.869	0.799	0.938	0.823	0.948	0.027	0.881	0.832	0.939	0.854	0.949	0.031	0.8837	<b>0.0350</b>
$L5$	0.864	0.834	0.929	0.854	0.939	0.048	0.868	0.797	0.936	0.821	0.946	0.027	0.881	0.832	0.938	0.852	0.948	0.031	0.8826	0.0353
$L4 + \epsilon$	0.864	0.836	0.929	0.857	0.94	0.047	0.869	0.799	0.937	0.824	0.947	0.027	0.881	0.833	0.939	0.855	0.949	0.031	<b>0.8839</b>	<b>0.0350</b>

**Table 5:** Degradation of R-SAMPC for Adverse Parameters ( $\times 10^{-3}$ ). Roman numerals (e.g., I, II) indicate different adverse parameters. Larger absolute values are better.

Model-SAM	I	II	III	IV	V
<b>COMPromter(M)</b>	-3.2	-0.9	-0.5	-0.3	-0.3
<b>M+R-SAMPC</b>	-3.9	-2.2	-1.8	-1.1	-1.1
<b>R-SAMPC Gain</b>	-0.7	-1.3	-1.3	-0.8	-0.8
<b>Relative Gain</b>	-21.87%	-144.44%	-260.00%	-266.67%	-266.67%

h).  $M2$  uses R-SAMPC, and this phenomenon is alleviated in the feature map. The hollowing in the corresponding final prediction map is also partially compensated (see  $M2$  line of groups a, e, g and h). Some hollow segments are close to the edge, so R-SAMPC can also help to segment the edge (see group b, c, d and f). In addition, the structural soundness of the R-SAMPC module is demonstrated in Table 4. The module design gap of R-SAMPC is more subtle, and six more comprehensive indicators are adopted. The metrics added are mean F-measure ( $F_m$ ) and max enhanced-alignment measure ( $E_x$ ). The pioneering use of a single convolutional layer as dropout gives the largest improvement, which is 0.59% in terms of average positive index and 0.33% in terms of MAE. When the number of convolutional layers reaches four ( $L4$ ), the index reaches its peak. By adding the channel scaling, the average positive accuracy increases by 0.02% compared with  $L4$ . Therefore, the rationality and effectiveness of the R-SAMPC are demonstrated, confirming its suitability. To validate the mitigation effect of R-SAMPC on adverse parameters, we selected five parameters where COMPromter shows reduced degradation compared to SAM, and conducted a quantitative comparison with the mitigation achieved by R-SAMPC. Details are provided in Table 5.

**Effectiveness of TVM.** The effectiveness of TVM is demonstrated by the gap between  $M3$  and  $M2$ . It can be obtained from Figure 5 that for the positive indicators, the improvement brought by  $M3$  is not as large as the improvement brought by  $M2$  to  $M1$ . However, the improvement of  $M3$  also comprehensively exceeds all the accuracy of  $M2$ . The effectiveness of TVM is analyzed based on average metrics.  $M3$  achieves an average improvement of 0.4% in  $S_\alpha$ , 0.4% in  $F_\beta^\omega$ , 0.5% in  $E_\phi$  across three datasets. Specifically, the  $E_\phi$  has been improved by 0.6%, 0.5%, and 0.4% in the three datasets. The

**Table 6:** Enhancement of TVM for Advantageous Parameters ( $\times 10^{-3}$ ). Roman numerals indicate different parameters. Larger absolute values are better.

Models-SAM	I	II	III	IV	V
<b>COMPromter (M)</b>	0.171	0.103	0.027	0.028	0.045
<b>M+R-SAMPC</b>	0.366	0.048	0.004	0.032	0.066
<b>M+R-SAMPC+TVM</b>	0.465	0.073	0.027	0.054	0.070
<b>TVM Gain</b>	+0.099	+0.025	+0.023	+0.022	+0.004
<b>Relative Gain</b>	+27.05%	+52.08%	+575.00%	+68.75%	+6.06%

comparison between  $M3$  and  $M3^*$  demonstrates that TTT achieves a higher positive metrics compared to Mamba. This indicates that TTT has a stronger ability to focus on beneficial features. The role of TVM is to compensate for the side effects introduced by R-SAMPC. This side effect weakens the advantageous parameters. It can be observed from the feature map of  $M1$  and  $M2$  that R-SAMPC makes the overall response more balanced, though it introduces some erroneous responses. TVM extracts features on the basis of R-SAMPC to correct the error response (see  $M3$  line of d in Figure 6). To validate the enhancement effect of TVM on advantageous parameters, we selected five parameters where COMPromter outperforms SAM, and performed a quantitative comparison of the improvements brought by TVM. Details are provided in Table 6.

## 5 Conclusion

The paper proposes SAM-TTT, a novel SAM-based network designed to address the semantic deficiency that occurs when applying SAM to COD. SAM-TTT consists of R-SAMPC and TVM. It offers a new approach for applying SAM to COD, widening the Effect Distance between advantageous and adverse parameters. The state-of-the-art performance of SAM-TTT is demonstrated over 15 cutting-edge methods across multiple datasets. SAM-TTT is a groundbreaking step towards non-parametric weakening of adverse parameters in SAM, and serves as a foundational step in introducing Test-Time Training to computer vision. Improving the combination of weakening adverse ones and emphasizing advantageous ones remains a key area for further exploration. Broadly, this concept could extend to other large model applications in downstream tasks.

## Acknowledgments

This work was supported in part by the National Key Research and Development Program Project of China [grant no. 2024YFC3306902], in part by the National Natural Science Foundation of China [grant nos. U24A20242, 62475241, 62472312], and in part by the Zhejiang Provincial Natural Science Foundation [grant no. LDT23F02024F02].

## References

- [1] Vishal Asnani, Abhinav Kumar, Suya You, and Xiaoming Liu. 2023. PrObeD: Proactive object detection wrapper. *NeurIPS* 36 (2023), 77993–78005.
- [2] Huafeng Chen, Dian Shao, Guangqian Guo, and Shan Gao. 2024. Just a Hint: Point-Supervised Camouflaged Object Detection. In *ECCV*.
- [3] Huafeng Chen, Pengxu Wei, Guangqian Guo, and Shan Gao. 2024. SAM-COD: SAM-guided Unified Framework for Weakly-Supervised Camouflaged Object Detection. In *ECCV*.
- [4] Tianrun Chen, Lanyun Zhu, Chaotao Ding, Runlong Cao, Shangzhan Zhang, Yan Wang, Zejian Li, Lingyun Sun, Papa Mao, and Ying Zang. 2023. SAM Fails to Segment Anything? SAM-Adapter: Adapting SAM in Underperformed Scenes: Camouflage, Shadow, and More. *arXiv preprint arXiv:2304.09148* (2023).
- [5] Anthony C Copeland and Mohan M Trivedi. 1997. Models and metrics for signature strength evaluation of camouflaged targets. In *Algorithms for synthetic aperture radar imagery IV*, Vol. 3070. 194–199.
- [6] Deng-Ping Fan, Ming-Ming Cheng, Yun Liu, Tao Li, and Ali Borji. 2017. Structure-measure: A new way to evaluate foreground maps. In *ICCV*.
- [7] Deng-Ping Fan, Cheng Gong, Yang Cao, Bo Ren, Ming-Ming Cheng, and Ali Borji. 2018. Enhanced-alignment measure for binary foreground map evaluation. In *IJCAI*.
- [8] Deng-Ping Fan, Ge-Peng Ji, Ming-Ming Cheng, and Ling Shao. 2021. Concealed object detection. *IEEE TPAMI* 44, 10 (2021), 6024–6042.
- [9] Deng-Ping Fan, Ge-Peng Ji, Peng Xu, Ming-Ming Cheng, Christos Sakaridis, and Luc Van Gool. 2023. Advances in deep concealed scene understanding. *VI* 1, 1 (2023), 16.
- [10] Albert Gu and Tri Dao. 2023. Mamba: Linear-time sequence modeling with selective state spaces. *arXiv preprint arXiv:2312.00752* (2023).
- [11] Chumming He, Kai Li, Yachao Zhang, Longxiang Tang, Yulun Zhang, Zhenhua Guo, and Xiu Li. 2023. Camouflaged object detection with feature decomposition and edge reconstruction. In *CVPR*.
- [12] Chumming He, Kai Li, Yachao Zhang, Guoxia Xu, Longxiang Tang, Yulun Zhang, Zhenhua Guo, and Xiu Li. 2024. Weakly-supervised concealed object segmentation with sam-based pseudo labeling and multi-scale feature grouping. *NIPS* 36 (2024).
- [13] Jian Hu, Jiayi Lin, Shaogang Gong, and Weitong Cai. 2024. Relax Image-Specific Prompt Requirement in SAM: A Single Generic Prompt for Segmenting Camouflaged Objects. In *AAAI*.
- [14] Xiaobin Hu, Shuo Wang, Xuebin Qin, Hang Dai, Wenqi Ren, Donghao Luo, Ying Tai, and Ling Shao. 2023. High-resolution iterative feedback network for camouflaged object detection. In *AAAI*.
- [15] Xihang Hu, Xiaoli Zhang, Fasheng Wang, Jing Sun, and Fuming Sun. 2024. Efficient Camouflaged Object Detection Network Based on Global Localization Perception and Local Guidance Refinement. *IEEE TCSVT* (2024).
- [16] Ge-Peng Ji, Deng-Ping Fan, Yu-Cheng Chou, Dengxin Dai, Alexander Liniger, and Luc Van Gool. 2023. Deep gradient learning for efficient camouflaged object detection. *MIR* 20, 1 (2023), 92–108.
- [17] Ge-Peng Ji, Deng-Ping Fan, Peng Xu, Bowen Zhou, Ming-Ming Cheng, and Luc Van Gool. 2023. SAM struggles in concealed scenes—empirical study on “Segment Anything”. *SCIS* 66, 12 (2023), 226101.
- [18] Qi Jia, Shuilian Yao, Yu Liu, Xin Fan, Risheng Liu, and Zhongxuan Luo. 2022. Segment, magnify and reiterate: Detecting camouflaged objects the hard way. In *CVPR*.
- [19] Abbas Khan, Mustaqueen Khan, Wail Gueaieb, Abdulmotaleb El Saddik, Giulia De Masi, and Fakhri Karray. 2024. CamoFocus: Enhancing Camouflage Object Detection With Split-Feature Focal Modulation and Context Refinement. In *WACV*.
- [20] Alexander Kirillov, Eric Mintun, Nikhila Ravi, Hanzi Mao, Chloe Rolland, Laura Gustafson, Tete Xiao, Spencer Whitehead, Alexander C Berg, Wan-Yen Lo, et al. 2023. Segment anything. In *ICCV*.
- [21] Krishna Kumar Singh and Yong Jae Lee. 2017. Hide-and-seek: Forcing a network to be meticulous for weakly-supervised object and action localization. In *ICCV*.
- [22] Trung-Nghia Le, Tam V Nguyen, Zhongliang Nie, Minh-Triet Tran, and Akihiro Sugimoto. 2019. Anabanch network for camouflaged object segmentation. *CVIU* 184 (2019), 45–56.
- [23] Aixuan Li, Jing Zhang, Yunqiu Lv, Bowen Liu, Tong Zhang, and Yuchao Dai. 2021. Uncertainty-aware joint salient object and camouflaged object detection. In *CVPR*.
- [24] Xinran Liu, Lin Qi, Yuxuan Song, and Qi Wen. 2024. Depth awakens: A depth-perceptual attention fusion network for RGB-D camouflaged object detection. *Image and Vision Computing* 143 (2024), 104924.
- [25] Yu Liu, Haihang Li, Juan Cheng, and Xun Chen. 2023. MSCAF-Net: a general framework for camouflaged object detection via learning multi-scale context-aware features. *IEEE TCSVT* 33, 9 (2023), 4934–4947.
- [26] Yunqiu Lv, Jing Zhang, Yuchao Dai, Aixuan Li, Bowen Liu, Nick Barnes, and Deng-Ping Fan. 2021. Simultaneously localize, segment and rank the camouflaged objects. In *CVPR*.
- [27] Jun Ma, Yuting He, Feifei Li, Lin Han, Chenyu You, and Bo Wang. 2024. Segment anything in medical images. *Nature Communications* 15, 1 (2024), 654.
- [28] Ran Margolin, Lihai Zelnik-Manor, and Ayellet Tal. 2014. How to evaluate foreground maps?. In *CVPR*.
- [29] Youwei Pang, Xiaoqi Zhao, Tian-Zhu Xiang, Lihe Zhang, and Huchuan Lu. 2022. Zoom in and out: A mixed-scale triplet network for camouflaged object detection. In *CVPR*.
- [30] Youwei Pang, Xiaoqi Zhao, Tian-Zhu Xiang, Lihe Zhang, and Huchuan Lu. 2024. Zoomnext: A unified collaborative pyramid network for camouflaged object detection. *IEEE TPAMI* (2024).
- [31] Ke Sun, Zhongxi Chen, Xianming Lin, Xiaoshuai Sun, Hong Liu, and Rongrong Ji. 2025. Conditional Diffusion Models for Camouflaged and Salient Object Detection. *IEEE TPAMI* 47, 4 (2025), 2833–2848.
- [32] Yu Sun, Xinhao Li, Karan Dalal, Jiarui Xu, Arjun Vikram, Genghan Zhang, Yann Dubois, Xinlei Chen, Xiaolong Wang, Sanmi Koyejo, et al. 2024. Learning to (learn at test time): Rnns with expressive hidden states. *arXiv preprint arXiv:2407.04620* (2024).
- [33] Yujia Sun, Shuo Wang, Chenglizhao Chen, and Tian Zhu Xiang. 2022. Boundary-Guided Camouflaged Object Detection. In *IJCAI*.
- [34] Yanguang Sun, Chunyan Xu, Jian Yang, Hanyu Xuan, and Lei Luo. 2024. Frequency-spatial entanglement learning for camouflaged object detection. In *ECCV*.
- [35] Lv Tang, Haoke Xiao, and Bo Li. 2023. Can sam segment anything? when sam meets camouflaged object detection. *arXiv preprint arXiv:2304.04709* (2023).
- [36] Liqiong Wang, Jinyu Yang, Yanfu Zhang, Fangyi Wang, and Feng Zheng. 2024. Depth-Aware Concealed Crop Detection in Dense Agricultural Scenes. In *CVPR*.
- [37] Fengyang Xiao, Sujie Hu, Yuqi Shen, Chengyu Fang, Jinfei Huang, Chunming He, Longxiang Tang, Ziyun Yang, and Xiu Li. 2024. A survey of camouflaged object detection and beyond. *arXiv preprint arXiv:2408.14562* (2024).
- [38] Fan Yang, Qiang Zhai, Xin Li, Rui Huang, Ao Luo, Hong Cheng, and Deng-Ping Fan. 2021. Uncertainty-guided transformer reasoning for camouflaged object detection. In *ICCV*.
- [39] Zhenni Yu, Xiaoqin Zhang, Yi Bin, Guobao Xiao, et al. 2024. Exploring Deeper! Segment Anything Model with Depth Perception for Camouflaged Object Detection. In *ACM MM*.
- [40] Guanghui Yue, Shangjie Wu, Tianwei Zhou, Gang Li, Jie Du, Yu Luo, and Qiuping Jiang. 2025. Progressive Region-to-Boundary Exploration Network for Camouflaged Object Detection. *IEEE TMM* 27 (2025), 236–248. doi:10.1109/TMM.2024.3521761
- [41] Jing Zhang, Deng-Ping Fan, Yuchao Dai, Saeed Anwar, Fatemeh Saleh, Sadegh Alibakr, and Nick Barnes. 2021. Uncertainty inspired RGB-D saliency detection. *IEEE TPAMI* 44, 9 (2021), 5761–5779.
- [42] Jin Zhang, Ruifeng Zhang, Yanjiao Shi, Zhe Cao, Nian Liu, and Fahad Shahbaz Khan. 2024. Learning Camouflaged Object Detection from Noisy Pseudo Label. In *ECCV*.
- [43] Xiaoqin Zhang, Zhenni Yu, Li Zhao, Deng-Ping Fan, and Guobao Xiao. 2024. COMPromter: reconceptualized segment anything model with multiprompt network for camouflaged object detection. *SCIS* (2024).
- [44] Jinchao Zhu, Xiaoyu Zhang, Shuo Zhang, and Junnan Liu. 2021. Inferring camouflaged objects by texture-aware interactive guidance network. In *AAAI*.